Cite as: S. Zeng *et al.*, *Science* 10.1126/science.abi5484 (2021).

Hierarchical-morphology metafabric for scalable passive daytime radiative cooling

Shaoning Zeng[1]†, Sijie Pian[2]†, Minyu Su[1], Zhuning Wang[2], Maoqi Wu[1,3], Xinhang Liu[2], Mingyue Chen[3], Yuanzhuo Xiang[1], Jiawei Wu[1], Manni Zhang[1], Qingqing Cen[2], Yuwei Tang[2], Xianheng Zhou[2], Zhiheng Huang[1], Rui Wang[1], Alitenai Tunuhe[1], Xiyu Sun[3], Zhigang Xia[4], Mingwei Tian[5], Min Chen[6], Xiao Ma[7], Lvyun Yang[1], Jun Zhou[1], Huamin Zhou[8], Qing Yang[2], Xin Li[7], Yaoguang Ma[2]*, Guangming Tao[1]*

[1]Wuhan National Laboratory for Optoelectronics, Huazhong University of Science and Technology, Wuhan 430074, China. [2]State Key Laboratory of Modern Optical Instrumentation, College of Optical Science and Engineering, International Research Center for Advanced Photonics, Zhejiang University, Hangzhou 310058, China. [3]iFabric Lab, TD Energy, Inc., Weifang 261500, China. [4]State Key Laboratory of New Textile Materials and Advanced Processing Technologies, Wuhan Textile University, Wuhan 430200, China. [5]Research Center for Intelligent and Wearable Technology, College of Textiles and Clothing, State Key Laboratory of Bio-Fibers and Eco-Textiles, Intelligent Wearable Engineering Research Center of Qingdao, Qingdao University, Qingdao 266071, China. [6]Wuhan National Laboratory for Optoelectronics and School of Computer Science and Technology, Huazhong University of Science and Technology, Wuhan 430074, China. [7]State Key Laboratory of Biobased Fiber Manufacturing Technology, China Textile Academy, Beijing 110105, China. [8]State Key Laboratory of Material Processing and Die and Mould Technology, School of Materials Science and Engineering, Huazhong University of Science and Technology, Wuhan 430074, China.

†These authors contributed equally to this work.

***Corresponding author. Email: tao@hust.edu.cn (G.T.); mayaoguang@zju.edu.cn (Y.M.)**

Incorporating passive radiative cooling structures into personal thermal management technologies could effectively defend human against the intensifying global climate change. We show that large scale woven metafabrics can provide high emissivity (94.5%) in the atmospheric window and reflectivity (92.4%) in the solar spectrum because the hierarchical-morphology design of the randomly dispersed scatterers throughout the metafabric. Through scalable industrial textile manufacturing routes, our metafabrics exhibit excellent mechanical strength, waterproofness, and breathability for commercial clothing while maintaining efficient radiative cooling ability. Practical application tests demonstrated the human body covered by our metafabric could be cooled down ~4.8°C lower than that covered by commercial cotton fabric. The cost-effectiveness and high-performance of our metafabrics present great advantages for intelligent garments, smart textiles, and passive radiative cooling applications.

As global warming intensifies, people exposed to outdoor environments are more at risk of illnesses related to excessive heat stress (*1*, *2*). Personal thermal management (PTM), a technology that controls the microclimate of the human body, can achieve thermal comfort with high efficiency (*3*). However, the key issues of energy consuming and bulky nature of current PTM design have not been solved yet (*4*–*7*). Radiative cooling, which radiates heat directly to outer space through the atmospheric transparent spectral window (ATSW, λ ~8 to 13 μm) (*8*, *9*), is a promising cooling method for overcoming these obstacles. Methods that harness nanophotonic structures like multilayer photonic structures (*9*, *10*), metamaterials (*11*, *12*), and random medium (*13*–*20*) have successfully yielded daytime radiative cooling devices and systems by simultaneously introducing solar irradiance rejection and enhancing the emitted thermal radiation. However, most radiative cooling structures (thin-films, coatings, paints, etc.) still result in weak air/water permeability and inadequate wearability properties that limit these materials from being directly applied to PTM systems (*21*). Thus, as the dominant medium that protects the skin from the external environment, clothing might be the perfect candidate to be implemented with daytime radiative cooling functionality.

Researchers have tested various types of mid-infrared (MIR)–transparent radiative cooling textiles (*22*–*26*). But, to maintain enough MIR transmittance, the thickness of the MIR-transparent structure is highly restricted to less than ~150 μm. Solar heating blockage and structural toughness become challenging at this thickness level. In contrast, the performance of MIR-emissive textiles does not depend on the spectrum of the underlying surface, thus relaxes the thickness restrictions. However, only few studies on MIR-emissive radiative cooling textiles or fibers have been proposed for PTM (*27*, *28*).

We designed a multilayer metafabric knitted with composite microfibers, which incorporates hierarchically designed random metamaterial structures to directly integrate radiative cooling technology for PTM applications. The hierarchical-morphology design mechanism directly provides an extended spectroscopic response that spans two orders of magnitude in wavelength (0.3 to 25 μm) and enables the metafabric to resonantly reject the solar power and strongly emit

in the MIR range (Fig. 1, A and B). The multilayer metafabric consists of a titanium oxide-polylactic acid (TiO_2-PLA) composite woven textile laminated with a thin polytetrafluoroethylene (PTFE) layer. The laminated top-layer is designed as a 50-μm-thick PTFE clothing film that is commercially available and widely used in clothing industries. The porous composite contains nanobeads of 200 to 1000 nm in size and nanofibers with length of several micron and width less than 200 nm (fig. S1). The composite strongly reflects ultraviolet (UV) light from the incoming radiation before it reaches the metatextile layer. As high-refractive-index scatterers, TiO_2 nanoparticles with size distributions between 200 and 1600 nm can utilize the collective effect of multiple Mie resonances (*29*, *30*) and produce scattering peaks required to cover the entire visible-near-infrared (VIS-NIR) band with high efficiency.

Selective emitters are desirable for radiative cooling applications when the working temperature is below ambient. For above ambient temperature scenarios, effective emission in the full MIR band can be useful. Therefore, PLA microfibers, which possess C=O (1825 to 1725 cm^{-1}), -CH_3 (1454.49 cm^{-1}), -CH (1382 to 1300 cm^{-1}), C-O (1042 to 1267 cm^{-1}), and C-C (867.67 cm^{-1}) bonds (*31*), were selected to provide rich emittance in the MIR waveband (fig. S2). Also, PLA fibers exhibit excellent solar transmittance, high moisture absorption properties, as well as remarkable biodegradability (*32*). The diameter of the fibers is designed to be ~30 μm for enhanced MIR absorption/emissivity (fig. S3), simultaneously exhibiting multiple scattering for increased absorption (*33*), and a rugged textile surface for gradient refractive index antireflection (*14*, *34*).

We further optimized the radiative cooling performance using a numerical model based on Lorenz-Mie theory and Monte Carlo simulations (*29*, *35*, *36*). The optical properties described by the pathlength-dependent electromagnetic scattering process between incoming radiation and metafabric requires more structure parameters to be rigorously determined to improve the radiative cooling capability of the metafabric. We selected nanoparticles with a log-normal distribution ($\mu = 6.2$, $\sigma^2 = 0.2$) and peak diameters of 400 nm (fig. S4) because they induced the best solar rejection performance enhancement of the fabric (Fig. 1C). Such a wide distribution of nanoparticles, when combined with PTFE nanobeads, provides broad-spectrum scattering and reflectivity across the UV-VIS-NIR band (Fig. 1D). We numerically evaluated the radiative cooling performance of the metafabric using a steady-state heat transfer model of clothed human skin with a skin temperature of 34°C and an ambient temperature of 22°C (*36*). We observed a net cooling power plateau corresponding to the thickness range of 400 to 600 μm, with the most efficient cooling behavior occurring at approximately 500 μm (Fig. 1E).

Modern fabrication technologies enabled great flexibility for the scalable manufacture of our metafabrics by realizing the hierarchical-morphology design at the sub-fiber level (Fig. 2A) (*36*). The metafibers (Fig. 2B) exhibited superior tensile properties with an elongation of 29.5% and a breakage strength of 1.886 cN/dtex (Fig. 2C), which are flexible and strong enough to be stitched and embroidered via a commercial sewing machine (Fig. 2D and movie S1). This compatibility with commercial sewing techniques allows the cooling metafibers to be applied to any clothing type and textile pattern. Mechanical tests showed that our metafabric (Fig. 2E and movie S2) can endure a tensile force of ~482 N and an elongation of ~20%, which are comparable to the mechanical properties of other commercial fabrics (Fig. 2F). The hydrophobic top surface of the metafabric exhibits excellent waterproofness (Fig. 2G), while the metafabric still maintains a certain degree of air permeability. When sandwiched between air and water environments, our metafabric exhibits continuous bubble transmittance and tight waterproofness that facilitates conventional heat exchange mechanisms for favorable wearability (Fig. 2H). The durability and washing resistance of our metafabric was also validated and suggests our technology is readily compatible with commercial applications (fig. S5) (*36*). Benefitting from our hierarchical-morphology design, the fabric shows a broadband reflectivity of 92.4% in the solar radiation region (0.3 to 2.5 μm) and an average emissivity of 94.5% across the ATSW (Fig. 2I). The broadband of high emissivity between 4 and 25 μm can provide additional cooling power for the working temperatures of our metafabric are higher than the ambient when used in PTM scenarios (*8*).

We demonstrated the outdoor radiative cooling performance of our metafabric by direct thermal measurements under clear sky conditions in Guangzhou, China (Fig. 3, A and B) (*36*). The temperature of each fabric sample was monitored by 3 K-type thermocouples taped on the copper plate to ensure the accuracy and uniformity of thermal measurements (Fig. 3C). Throughout a continuous 24-hour measurement period, the metafabric consistently maintained a temperature below the ambient temperature (Fig. 3D). The minimum temperature difference was ~2°C, which occurred within half an hour of the peak solar irradiance. Furthermore, we tested the radiative cooling performance of our metafabric on a human skin simulator (Fig. 3E) (*36*). Under peak solar irradiance between 11:00 and 15:00, the temperature of the metafabric was approximately 5.0°, 6.8°, 7.0°, 5.8°, and 10.2°C lower than that of the cotton, spandex, chiffon, linen, and bare skin simulators, respectively (Fig. 3F).

To validate the cooling performance of our metafabric with scalable, wearable features in pragmatic scenarios, we composed a homemade vest by sewing a commercial cotton fabric and a metafabric together. A volunteer wearing that

vest reclined under direct sunlight for an hour while we monitored the thermal properties of the vest and the volunteer (Fig. 4A). Thermal camera (Fluke Ti400) showed a large temperature difference between the two sides of the vest (34.4° and 31.0°C). Thermocouples adhered under the vest also indicated a temperature difference of ~4.8°C between the parts of the body that were covered by different fabrics (Fig. 4B). A similar test for the radiative cooling vest was performed in Sipsongpanna, China, for repeatability. During the half-hour measurement process, the surface of each half of the vest gradually exhibited a notable temperature difference (Fig. 4C and movie S3). Amazingly, the two halves of the body showed a distinct temperature difference of more than 3°C right after the vest was removed. In addition, we tested the cooling performance of the metafabric with three car models covered by a commercial vehicle cover (*36*), our metafabric, and nothing, respectively (Fig. 4A). During a 90-min experiment, the maximum interior temperature of the car model covered by the metafabric was ~30° and ~27°C cooler than that of the models with no cover and with a vehicle cover, respectively (Fig. 4D). These results show the great potential for commercial applications in various complex scenarios, such as smart textiles, sunshade products, logistics transportation, etc. (fig. S6).

The metafabric exhibits efficient radiative cooling performance and provides necessary breathability and wearing comfort for PTM. Compared with passive cooling routes like films or paints, the woven structure enables metafabric to easily accommodate complex deformations (bending, stretching and twisting), which leads to versatile compatibility. Through embroidery, cutting and sewing, the metafabric can be integrated into various products for different scenarios, such as clothing, tents, car covers, curtains and awnings. Further optimization and exploration of the fiber structural features are expected to improve the cooling efficiency by the combined effect of both radiative cooling and perspiration evaporation (*37*). Although we have not yet explored the color compatible radiative cooling and cooling power modulation of the metafabric, based on the idea of hierarchical-morphology design, applying a fourth level dyeing layer and adopting asymmetrical photonics structures may address above challenges.

REFERENCES AND NOTES

1. R. A. I. Lucas, Y. Epstein, T. Kjellstrom, Excessive occupational heat exposure: A significant ergonomic challenge and health risk for current and future workers. *Extrem. Physiol. Med.* **3**, 14 (2014). doi:10.1186/2046-7648-3-14 Medline
2. L. T. Biardeau, L. W. Davis, P. Gertler, C. Wolfram, Heat exposure and global air conditioning. *Nat. Sustain.* **3**, 25–28 (2020). doi:10.1038/s41893-019-0441-9
3. Y. Peng, Y. Cui, Advanced textiles for personal thermal management and energy. *Joule* **4**, 724–742 (2020). doi:10.1016/j.joule.2020.02.011
4. M. Zhao, C. Gao, F. Wang, K. Kuklane, I. Holmér, J. Li, A study on local cooling of garments with ventilation fans and openings placed at different torso sites. *Int. J. Ind. Ergon.* **43**, 232–237 (2013). doi:10.1016/j.ergon.2013.01.001
5. T. Gao, Z. Yang, C. Chen, Y. Li, K. Fu, J. Dai, E. M. Hitz, H. Xie, B. Liu, J. Song, B. Yang, L. Hu, Three-dimensional printed thermal regulation textiles. *ACS Nano* **11**, 11513–11520 (2017). doi:10.1021/acsnano.7b06295 Medline
6. T. Zhang, K. Li, J. Zhang, M. Chen, Z. Wang, S. Ma, N. Zhang, L. Wei, High-performance, flexible, and ultralong crystalline thermoelectric fibers. *Nano Energy* **41**, 35–42 (2017). doi:10.1016/j.nanoen.2017.09.019
7. D. Zhao, X. Lu, T. Fan, Y. S. Wu, L. Lou, Q. Wang, J. Fan, R. Yang, Personal thermal management using portable thermoelectrics for potential building energy saving. *Appl. Energy* **218**, 282–291 (2018). doi:10.1016/j.apenergy.2018.02.158
8. D. Zhao, A. Aili, Y. Zhai, S. Xu, G. Tan, X. Yin, R. Yang, Radiative sky cooling: Fundamental principles, materials, and applications. *Appl. Phys. Rev.* **6**, 021306 (2019). doi:10.1063/1.5087281
9. A. P. Raman, M. A. Anoma, L. Zhu, E. Rephaeli, S. Fan, Passive radiative cooling below ambient air temperature under direct sunlight. *Nature* **515**, 540–544 (2014). doi:10.1038/nature13883 Medline
10. Z. Chen, L. Zhu, A. Raman, S. Fan, Radiative cooling to deep sub-freezing temperatures through a 24-h day–night cycle. *Nat. Commun.* **7**, 13729 (2016). doi:10.1038/ncomms13729 Medline
11. M. M. Hossain, B. Jia, M. Gu, A metamaterial emitter for highly efficient radiative cooling. *Adv. Opt. Mater.* **3**, 1047–1051 (2015). doi:10.1002/adom.201500119
12. Y. Zhai, Y. Ma, S. N. David, D. Zhao, R. Lou, G. Tan, R. Yang, X. Yin, Scalable-manufactured randomized glass-polymer hybrid metamaterial for daytime radiative cooling. *Science* **355**, 1062–1066 (2017). doi:10.1126/science.aai7899 Medline
13. Z. Huang, X. Ruan, Nanoparticle embedded double-layer coating for daytime radiative cooling. *Int. J. Heat Mass Transf.* **104**, 890–896 (2017). doi:10.1016/j.ijheatmasstransfer.2016.08.009
14. J. Mandal, Y. Fu, A. C. Overvig, M. Jia, K. Sun, N. N. Shi, H. Zhou, X. Xiao, N. Yu, Y. Yang, Hierarchically porous polymer coatings for highly efficient passive daytime radiative cooling. *Science* **362**, 315–319 (2018). doi:10.1126/science.aat9513 Medline
15. T. Li, Y. Zhai, S. He, W. Gan, Z. Wei, M. Heidarinejad, D. Dalgo, R. Mi, X. Zhao, J. Song, J. Dai, C. Chen, A. Aili, A. Vellore, A. Martini, R. Yang, J. Srebric, X. Yin, L. Hu, A radiative cooling structural material. *Science* **364**, 760–763 (2019). doi:10.1126/science.aau9101 Medline
16. D. Li, X. Liu, W. Li, Z. Lin, B. Zhu, Z. Li, J. Li, B. Li, S. Fan, J. Xie, J. Zhu, Scalable and hierarchically designed polymer film as a selective thermal emitter for high-performance all-day radiative cooling. *Nat. Nanotechnol.* **16**, 153–158 (2021). doi:10.1038/s41565-020-00800-4 Medline
17. X. Li, J. Peoples, Z. Huang, Z. Zhao, J. Qiu, X. Ruan, Full daytime sub-ambient radiative cooling in commercial-like paints with high figure of merit. *Cell Rep. Phys. Sci.* **1**, 100221 (2020). doi:10.1016/j.xcrp.2020.100221
18. J. Mandal, Y. Yang, N. Yu, A. P. Raman, Paints as a scalable and effective radiative cooling technology for buildings. *Joule* **4**, 1350–1356 (2020). doi:10.1016/j.joule.2020.04.010
19. X. Xue, M. Qiu, Y. Li, Q. M. Zhang, S. Li, Z. Yang, C. Feng, W. Zhang, J.-G. Dai, D. Lei, W. Jin, L. Xu, T. Zhang, J. Qin, H. Wang, S. Fan, Creating an eco-friendly building coating with smart subambient radiative cooling. *Adv. Mater.* **32**, e1906751 (2020). doi:10.1002/adma.201906751 Medline
20. T. Wang, Y. Wu, L. Shi, X. Hu, M. Chen, L. Wu, A structural polymer for highly efficient all-day passive radiative cooling. *Nat. Commun.* **12**, 365 (2021). doi:10.1038/s41467-020-20646-7 Medline
21. W. Yan, C. Dong, Y. Xiang, S. Jiang, A. Leber, G. Loke, W. Xu, C. Hou, S. Zhou, M. Chen, R. Hu, P. P. Shum, L. Wei, X. Jia, F. Sorin, X. Tao, G. Tao, Thermally drawn advanced functional fibers: New frontier of flexible electronics. *Mater. Today* **35**, 168–194 (2020). doi:10.1016/j.mattod.2019.11.006
22. J. K. Tong, X. Huang, S. V. Boriskina, J. Loomis, Y. Xu, G. Chen, Infrared-transparent visible-opaque fabrics for wearable personal thermal management. *ACS Photonics* **2**, 769–778 (2015). doi:10.1021/acsphotonics.5b00140
23. P.-C. Hsu, A. Y. Song, P. B. Catrysse, C. Liu, Y. Peng, J. Xie, S. Fan, Y. Cui, Radiative human body cooling by nanoporous polyethylene textile. *Science* **353**, 1019–1023 (2016). doi:10.1126/science.aaf5471 Medline
24. L. Cai, A. Y. Song, W. Li, P.-C. Hsu, D. Lin, P. B. Catrysse, Y. Liu, Y. Peng, J. Chen, H. Wang, J. Xu, A. Yang, S. Fan, Y. Cui, Spectrally selective nanocomposite textile for outdoor personal cooling. *Adv. Mater.* **30**, e1802152 (2018). doi:10.1002/adma.201802152 Medline

25. Y. Peng, J. Chen, A. Y. Song, P. B. Catrysse, P.-C. Hsu, L. Cai, B. Liu, Y. Zhu, G. Zhou, D. S. Wu, H. R. Lee, S. Fan, Y. Cui, Nanoporous polyethylene microfibres for large-scale radiative cooling fabric. *Nat. Sustain.* **1**, 105–112 (2018). doi:10.1038/s41893-018-0023-2
26. L. Cai, Y. Peng, J. Xu, C. Zhou, C. Zhou, P. Wu, D. Lin, S. Fan, Y. Cui, Temperature regulation in colored infrared-transparent polyethylene textiles. *Joule* **3**, 1478–1486 (2019). doi:10.1016/j.joule.2019.03.015
27. X. A. Zhang, S. Yu, B. Xu, M. Li, Z. Peng, Y. Wang, S. Deng, X. Wu, Z. Wu, M. Ouyang, Y. Wang, Dynamic gating of infrared radiation in a textile. *Science* **363**, 619–623 (2019). doi:10.1126/science.aau1217 Medline
28. N. N. Shi, C.-C. Tsai, M. J. Carter, J. Mandal, A. C. Overvig, M. Y. Sfeir, M. Lu, C. L. Craig, G. D. Bernard, Y. Yang, N. Yu, Nanostructured fibers as a versatile photonic platform: Radiative cooling and waveguiding through transverse Anderson localization. *Light Sci. Appl.* **7**, 37 (2018). doi:10.1038/s41377-018-0033-x Medline
29. H. C. van de Hulst, *Light Scattering by Small Particles* (Courier Corporation, 1981).
30. P. Chýlek, J. Zhan, Interference structure of the Mie extinction cross section. *J. Opt. Soc. Am. A* **6**, 1846–1851 (1989). doi:10.1364/JOSAA.6.001846
31. Ł. Łopusiewicz, F. Jędra, M. Mizielińska, New poly(lactic acid) active packaging composite films incorporated with fungal melanin. *Polymers* **10**, 386 (2018). doi:10.3390/polym10040386 Medline
32. N. F. Zaaba, M. Jaafar, A review on degradation mechanisms of polylactic acid: Hydrolytic, photodegradative, microbial, and enzymatic degradation. *Polym. Eng. Sci.* **60**, 2061–2075 (2020). doi:10.1002/pen.25511
33. R. Mupparapu, K. Vynck, T. Svensson, M. Burresi, D. S. Wiersma, Path length enhancement in disordered media for increased absorption. *Opt. Express* **23**, A1472–A1484 (2015). doi:10.1364/OE.23.0A1472 Medline
34. H. Zhang, K. C. S. Ly, X. Liu, Z. Chen, M. Yan, Z. Wu, X. Wang, Y. Zheng, H. Zhou, T. Fan, Biologically inspired flexible photonic films for efficient passive radiative cooling. *Proc. Natl. Acad. Sci. U.S.A.* **117**, 14657–14666 (2020). doi:10.1073/pnas.2001802117 Medline
35. L. Wang, S. L. Jacques, L. Zheng, MCML—Monte Carlo modeling of light transport in multi-layered tissues. *Comput. Methods Programs Biomed.* **47**, 131–146 (1995). doi:10.1016/0169-2607(95)01640-F Medline
36. Materials and methods are available as supplementary materials.
37. R. K. Varshney, V. K. Kothari, S. Dhamija, A study on thermophysiological comfort properties of fabrics in relation to constituent fibre fineness and cross-sectional shapes. *J. Textil. Inst.* **101**, 495–505 (2010). doi:10.1080/00405000802542184
38. K. Laaksonen, S. Y. Li, S. R. Puisto, N. K. J. Rostedt, T. Ala-Nissila, C. G. Granqvist, R. M. Nieminen, G. A. Niklasson, Nanoparticles of TiO_2 and VO_2 in dielectric media: Conditions for low optical scattering, and comparison between effective medium and four-flux theories. *Sol. Energy Mater. Sol. Cells* **130**, 132–137 (2014). doi:10.1016/j.solmat.2014.06.036
39. The Solcast API Toolkit (2020); https://toolkit.solcast.com.au/live-forecast.
40. C. F. Bohren, D. R. Huffman, *Absorption and Scattering of Light by Small Particles* (John Wiley & Sons, 1983).
41. J. Yin, L. Pilon, Efficiency factors and radiation characteristics of spherical scatterers in an absorbing medium. *J. Opt. Soc. Am. A Opt. Image Sci. Vis.* **23**, 2784–2796 (2006). doi:10.1364/JOSAA.23.002784 Medline
42. M. F. Modest, *Radiative Heat Transfer* (Academic Press, 2013).
43. M. S. Wheeler, J. S. Aitchison, J. I. L. Chen, G. A. Ozin, M. Mojahedi, Infrared magnetic response in a random silicon carbide micropowder. *Phys. Rev. B* **79**, 073103 (2009). doi:10.1103/PhysRevB.79.073103
44. W. C. Smith, *Smart Textile Coatings and Laminates* (Woodhead Publishing, 2010).
45. J. Song, J. Qin, J. Qu, Z. Song, W. Zhang, X. Xue, Y. Shi, T. Zhang, W. Ji, R. Zhang, H. Zhang, Z. Zhang, X. Wu, The effects of particle size distribution on the optical properties of titanium dioxide rutile pigments and their applications in cool non-white coatings. *Sol. Energy Mater. Sol. Cells* **130**, 42–50 (2014). doi:10.1016/j.solmat.2014.06.035

ACKNOWLEDGMENTS

The authors would like to acknowledge Xinliang Zhang and Jiwen Liu for his encouragement, support, and vision. We thank Professor Xu Liu for his helpful discussion, Pengfei Wu for assistance with the melt-spinning experiment, Cancan Wang and Kai Wang for assistance with textile weaving, and Yulong Ma, Shuya Zhao, and Wenling Chen for performing the experimental measurements. **Funding:** This work was supported by the National Natural Science Foundation of China (G.T. grant no. 61875064 and Y.M. grant no. 61905213). **Author contributions:** G.T. and Y.M. conceived of the idea, designed the experiments and supervised the research project. S.Z. and S.P. conducted the experiments. S.Z. performed the manufacturing and characterization of the fibers and fabrics. S.P. performed the modeling and simulation. G.T., Y.M., S.Z., and S.P. analyzed the data and wrote the paper. All authors contributed to the experiments and discussion of the manuscript. **Competing interests:** The authors declare that they have no competing interests. **Data and materials availability:** All data are available in the main text or the supplementary materials. Information requests should be directed to the corresponding authors.

SUPPLEMENTARY MATERIALS

science.sciencemag.org/cgi/content/full/science.abi5484/DC1
Materials and Methods
Supplementary Text
Figs. S1 to S10
Tables S1 and S2
References (*38*–*45*)
Movies S1 to S6

16 March 2021; accepted 28 June 2021
Published online 8 July 2021
10.1126/science.abi5484

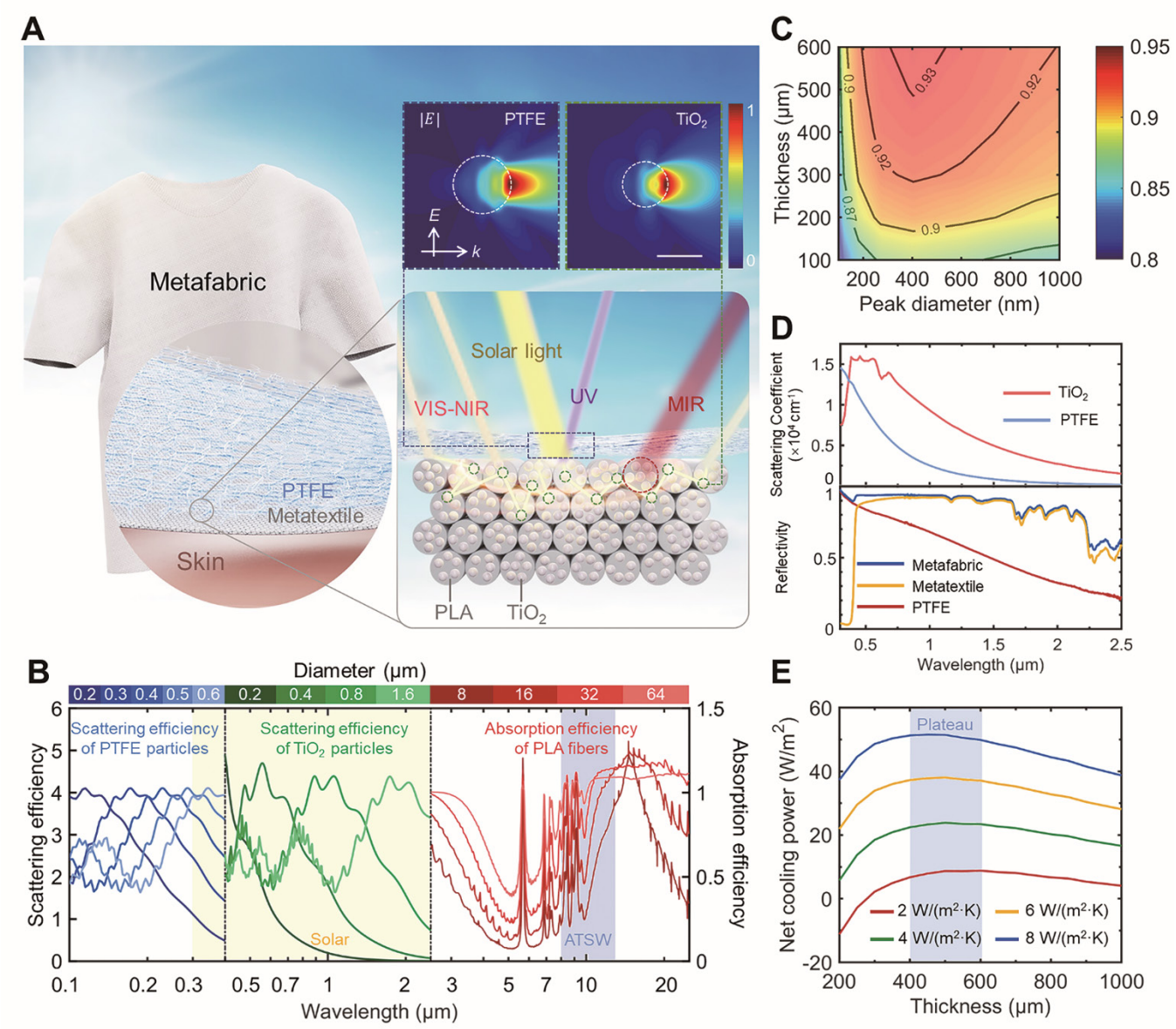

Fig. 1. Proposed structure and simulated properties of the metafabric. (**A**) Schematic of a metafabric for daytime radiative cooling. The blue, green and red dashed boxes highlight the three-level hierarchical structure responding to the UV, VIS-NIR and MIR bands, respectively. The insets show the calculated scattering fields of 300 nm and 550 nm light by a 500 nm PTFE particle and a 400 nm TiO_2 particle, respectively. Scale bar, 400 nm. (**B**) Calculated scattering and absorption efficiencies for particles with different sizes encapsulated in the metafabric. PTFE particles, TiO_2 particles and PLA fibers demonstrate strong scattering/absorption of UV light, VIS-NIR light and MIR light, respectively. (**C**) Calculated solar reflectance (0.3 to 2.5 μm) of the metafabric with different thicknesses and TiO_2 particle sizes under the same doping concentration (15% volume fraction). For a consistent thickness, the log-normal distribution of TiO_2 particles with a peak diameter of 400 nm (μ = 6.2, σ^2 = 0.2) can provide the highest solar reflectance. (**D**) Upper, scattering coefficients of PTFE and TiO_2 nanoparticles with optimized size distributions and volume fractions of 15%. Lower, measured solar radiation band reflectivity curves of metafabric, metatextile, and PTFE clothing films. (**E**) Calculated net cooling power of the metafabric vs. fabric thickness using different heat convection coefficients with a skin temperature of 34°C and an ambient temperature of 22°C.

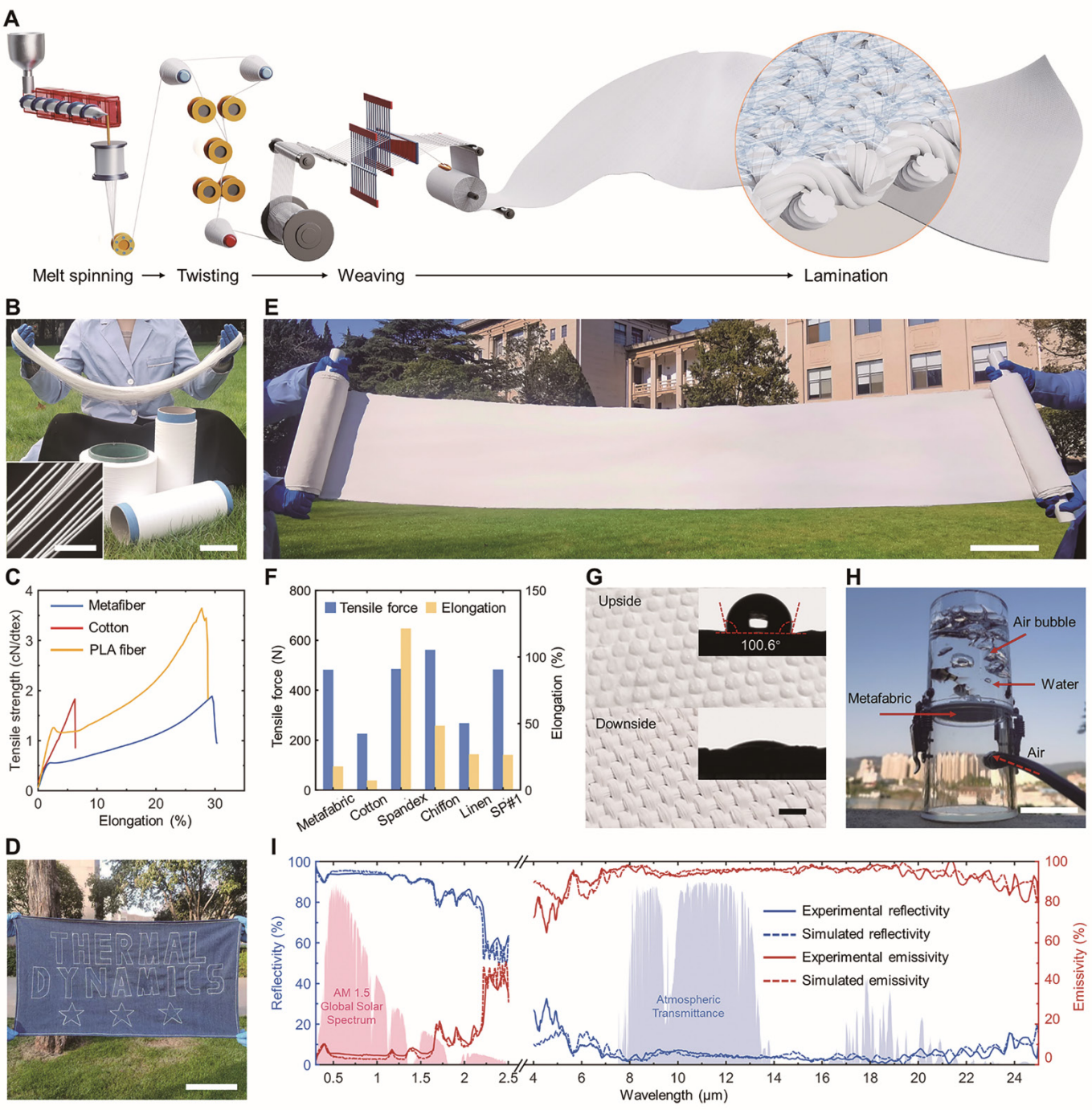

Fig. 2. Manufacture and characterization of the metafabric. (**A**) The fabrication process of the metafabric. (**B**) Photograph of the fabricated metafibers. Scale bar, 10 cm. The inset shows an optical micrograph of metafibers with diameters of ~30 μm. Scale bar, 500 μm. (**C**) Mechanical strength tests of the fiber strength versus elongation. (**D**) Photograph of metafibers embroidered with the letters "THERMAL DYNAMICS" on denim. Scale bar, 20 cm. (**E**) Photograph of the metafabric (0.3 m by 15 m). Scale bar, 20 cm. (**F**) A tensile strength test of the metafabric, cotton, spandex, chiffon, linen, and sun-protective clothing #1 (SP#1). (**G**) Morphologies of the upper and lower surfaces of the metafabric. The upper surface is hydrophobic, and the lower surface is hydrophilic, as shown in the insets contact angle tests. Scale bar, 1 mm. (**H**) Demonstration of the waterproofness and breathability of the metafabric. Scale bar, 5 cm. (**I**) Measured reflectivity and emissivity spectra of the metafabric (0.3 to 25 μm).

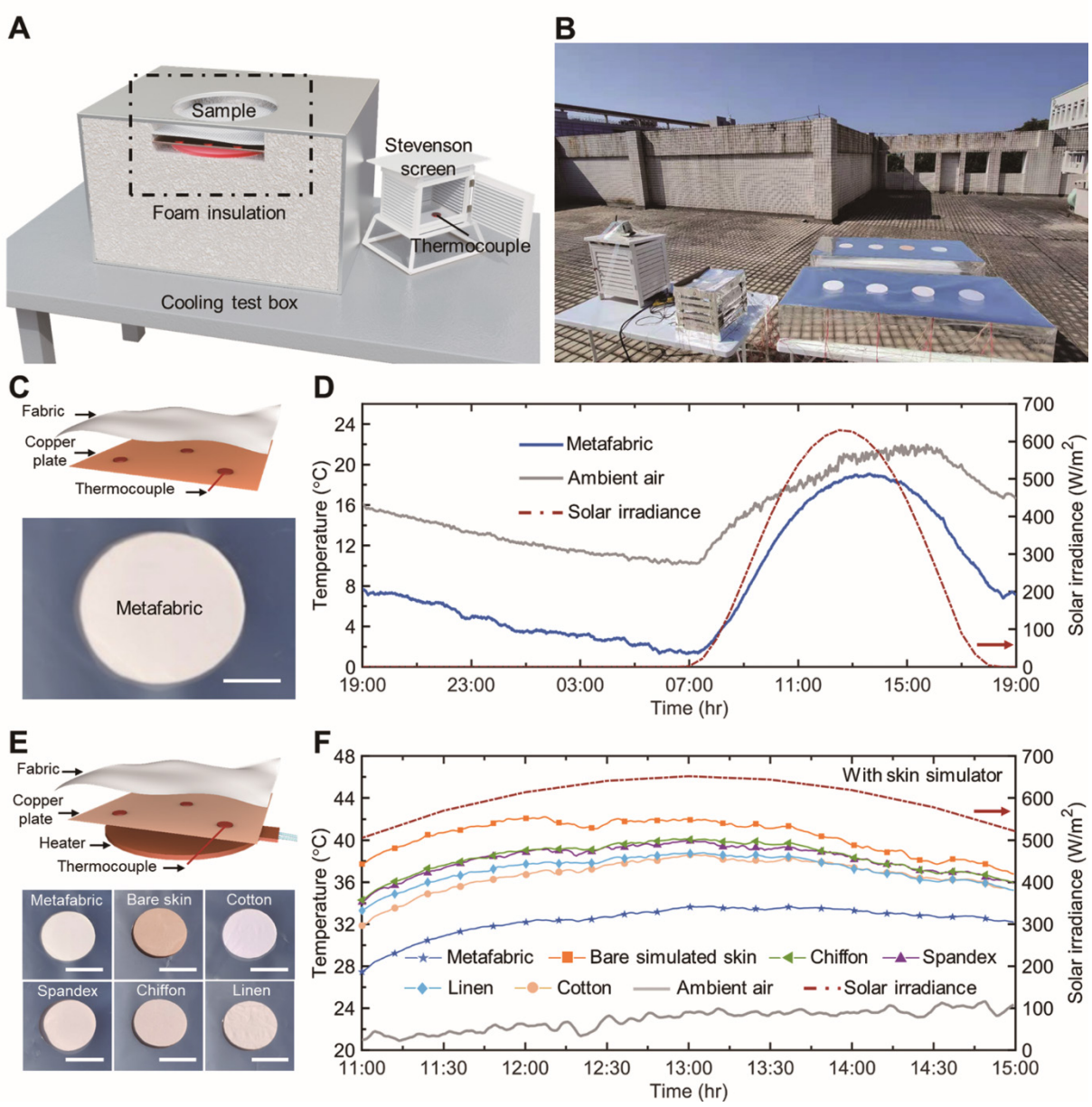

Fig. 3. Direct thermal analysis to determine the metafabric cooling performance. (**A**) Schematic and (**B**) photo of the thermal measurement system used to characterize the radiative cooling performance. (**C**) Schematic and photo of the sample structure for the test. Scale bar, 5 cm. (**D**) A 24-hour continuous temperature measurement of the subambient cooling performance test in Guangzhou, China (23°5′32″N, 113°23′45″E, December 5-6, 2020). (**E**) Schematic of the device used for the skin simulator cooling test and photographs of the fabric samples used in the test. Scale bars, 10 cm. (**F**) Temperature difference of skin simulators under different fabric samples in same location (November 28, 2020).

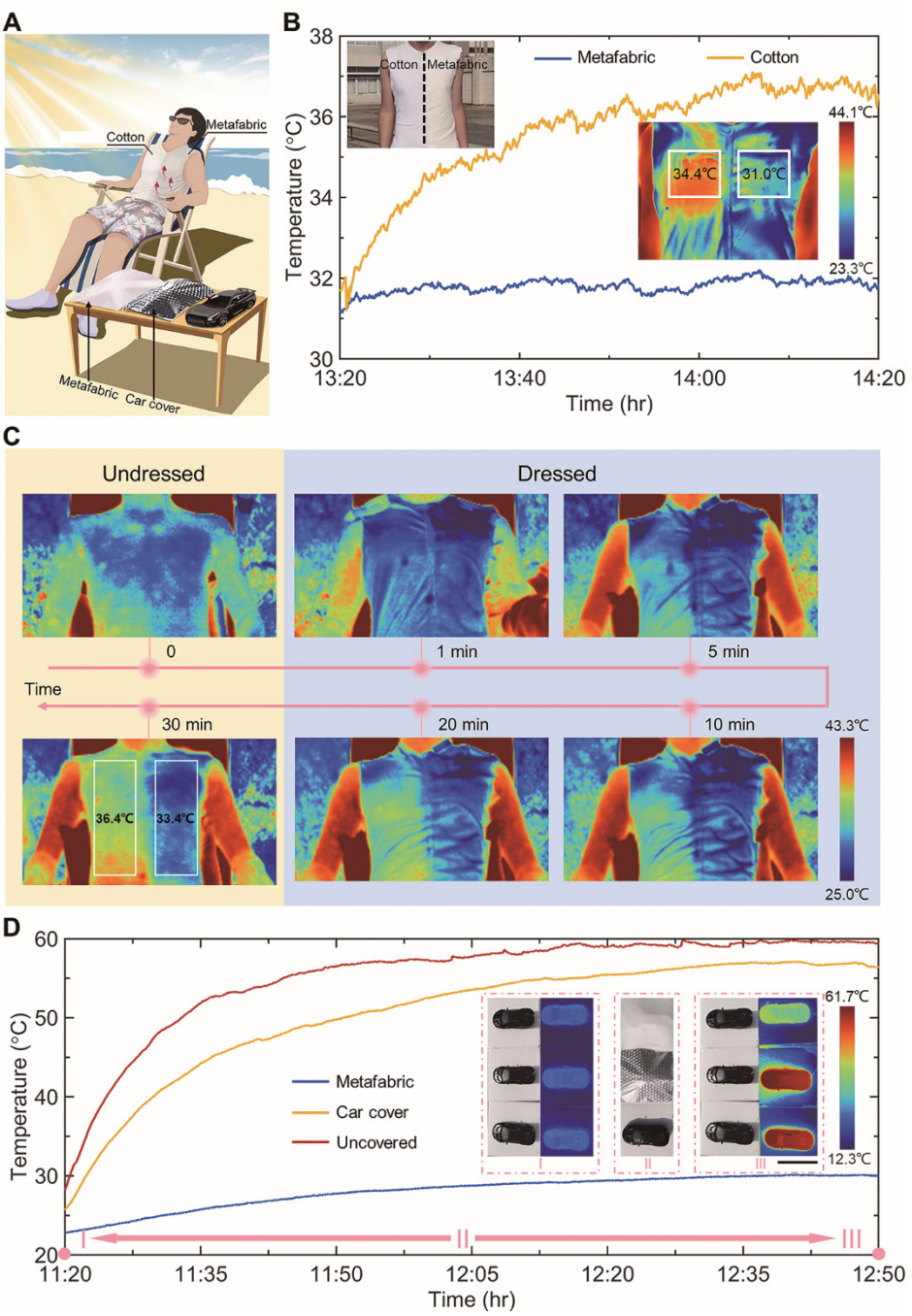

Fig. 4. Practical characterization of the metafabric with sun exposure. (**A**) Schematic of the metafabric cooling tests on the human body and model cars. (**B**) Temperature tracking for skin under different fabrics in direct sunlight in Guangzhou, China (23°5′32″N, 113°23′45″E, December 7, 2020). The insets show photographs and thermal images of the volunteer wearing a homemade vest. (**C**) Infrared images of the volunteer under direct sunlight in Sipsongpanna, China (22°10′22″N, 100°51′29″E, December 13, 2020). (**D**) Temperature test curves of three identical car models exposed to the sun. The inset shows photographs and IR images of the car models during the three time periods. "I" and "III" labels correspond to the initial and final measurements, respectively, and "II" shows a photograph of the whole test process. Scale bar, 10 cm.

Hierarchical-morphology metafabric for scalable passive daytime radiative cooling

Shaoning Zeng, Sijie Pian, Minyu Su, Zhuning Wang, Maoqi Wu, Xinhang Liu, Mingyue Chen, Yuanzhuo Xiang, Jiawei Wu, Manni Zhang, Qingqing Cen, Yuwei Tang, Xianheng Zhou, Zhiheng Huang, Rui Wang, Alitenai Tunuhe, Xiyu Sun, Zhigang Xia, Mingwei Tian, Min Chen, Xiao Ma, Lvyun Yang, Jun Zhou, Huamin Zhou, Qing Yang, Xin Li, Yaoguang Ma and Guangming Tao

published online July 8, 2021